Self-Consistent Extraction of Spectroscopic Bounds on Light New Physics

Cédric Delaunay,[1,2,*] Jean-Philippe Karr,[3,4,†] Teppei Kitahara,[5,6,7,‡] Jeroen C. J. Koelemeij,[8,§]
Yotam Soreq,[9,∥] and Jure Zupan[10,¶]

[1]*Laboratoire d'Annecy-le-Vieux de Physique Théorique, CNRS—USMB, BP 110 Annecy-le-Vieux, F-74941 Annecy, France*
[2]*Theoretical Physics Department, CERN, Esplanade des Particules 1, Geneva CH-1211, Switzerland*
[3]*Laboratoire Kastler Brossel, Sorbonne Université, CNRS, ENS-Université PSL, Collège de France, 4 place Jussieu, F-75005 Paris, France*
[4]*Université d'Evry-Val d'Essonne, Université Paris-Saclay, Boulevard François Mitterrand, F-91000 Evry, France*
[5]*Institute for Advanced Research and Kobayashi-Maskawa Institute for the Origin of Particles and the Universe, Nagoya University, Nagoya 464–8602, Japan*
[6]*KEK Theory Center, IPNS, KEK, Tsukuba 305–0801, Japan*
[7]*CAS Key Laboratory of Theoretical Physics, Institute of Theoretical Physics, Chinese Academy of Sciences, Beijing 100190, China*
[8]*LaserLaB, Department of Physics and Astronomy, Vrije Universiteit Amsterdam, De Boelelaan 1081, 1081 HV Amsterdam, Netherlands*
[9]*Physics Department, Technion—Israel Institute of Technology, Haifa 3200003, Israel*
[10]*Department of Physics, University of Cincinnati, Cincinnati, Ohio 45221,USA*

(Received 31 October 2022; accepted 3 March 2023; published 24 March 2023)

Fundamental physical constants are determined from a collection of precision measurements of elementary particles, atoms, and molecules. This is usually done under the assumption of the standard model (SM) of particle physics. Allowing for light new physics (NP) beyond the SM modifies the extraction of fundamental physical constants. Consequently, setting NP bounds using these data, and at the same time assuming the Committee on Data of the International Science Council recommended values for the fundamental physical constants, is not reliable. As we show in this Letter, both SM and NP parameters can be simultaneously determined in a consistent way from a global fit. For light vectors with QED-like couplings, such as the dark photon, we provide a prescription that recovers the degeneracy with the photon in the massless limit and requires calculations only at leading order in the small new physics couplings. At present, the data show tensions partially related to the proton charge radius determination. We show that these can be alleviated by including contributions from a light scalar with flavor nonuniversal couplings.

DOI: 10.1103/PhysRevLett.130.121801

Introduction.—Precision measurements of atomic and molecular properties play a dual role in fundamental physics. On the one hand, assuming the standard model (SM) of particle physics, these are used to determine two of the SM parameters, the fine-structure constant α and the electron mass m_e [through the Rydberg constant $R_\infty \equiv \alpha^2 m_e c/(2h)$], along with a number of other observables such as the charge radii and relative atomic masses of the proton and deuteron. An example is the determination of fundamental physical constants by the Committee on Data of the International Science Council (CODATA) [1].

On the other hand, precision measurements can be used to search for new physics (NP) beyond the SM. Such searches have been conducted using measurements of single particle observables [2–4], atomic systems [5–10], and molecular systems [11–14], see [15] for a review. The presence of NP would manifest itself as a discrepancy between measurements and theoretical SM predictions. The difficulty here is that in many cases the SM predictions depend on the fundamental physics parameters, which in turn were extracted from data by CODATA under the assumption that the SM is correct, and no NP exists. In general, the presence of NP would affect the extraction of fundamental constants, possibly reducing the claimed sensitivity of NP searches. This subtlety is more often than not ignored in the literature.

In this Letter, we propose and carry out a self-consistent determination of constraints on light NP models by performing a global fit, simultaneously extracting the SM and NP parameters. We go well beyond the previous studies [5,6,16], which were performed only on subsets of data. We pay special attention to the potentially problematic limit of massless NP. The challenge is that the SM predictions are calculated to a higher perturbative order than the leading-order (LO) NP contributions, which can then lead to incorrect limiting behavior for very light NP. Below, we provide a prescription, valid to LO in NP parameters, that corrects for such mismatches in the theoretical predictions and leads to the proper massless NP limit.

The global fit shows several 3σ (3 standard deviations) discrepancies between observables and predictions, assuming the SM. These anomalies are well known: they correspond to the measurements constituting the proton charge radius puzzle [17–19], with the addition of new measurements of hydrogen transitions [20,21]. Reference [20] showed the tension of their $2S_{1/2} - 8D_{5/2}$ measurement with other hydrogen data is relaxed in the presence of an additional Yukawa-like interaction. Our global analysis, which determines simultaneously both the SM and NP parameters, shows for the first time that all these deviations can be largely accounted for in a single NP model—a light scalar that couples to gluons, electrons, and muons.

New physics benchmark models.—We focus on minimal extensions of the SM, where either a light scalar boson ϕ or a light vector boson ϕ_μ is added to the spectrum of SM particles. The new light particle is assumed to have parity conserving interactions with the SM electrons and muons, as well as with light quarks, resulting in couplings to neutrons and protons. (Extension to parity nonconserving couplings and additional particles is straightforward.)

The interaction Lagrangian is therefore given by

$$\mathcal{L}_{\text{int}} = \sum_{i=e,\mu,n,p} g_i \bar{\psi}_i (\Gamma\phi) \psi_i, \tag{1}$$

where $\Gamma\phi \equiv \phi, \gamma^\mu \phi_\mu$ for spin $s = 0, 1$ bosons, respectively. Taking the nonrelativistic limit for ψ_i, and working at LO in g_i, the tree-level exchange of ϕ or ϕ_μ induces a Yukawa-like nonrelativistic potential,

$$V_{\text{NP}}^{ij}(r) = (-1)^{s+1} \alpha_\phi q_i q_j \frac{e^{-m_\phi r}}{r}, \tag{2}$$

between particles ψ_i and ψ_j, separated by a distance r. The NP coupling constant $\alpha_\phi \equiv |g_e g_p|/(4\pi) > 0$, gives the strength of the NP induced potential between electrons and protons. The strength of NP interactions between fermions ψ_i and ψ_j, relative to the electron-proton one, is given by the product of effective NP couplings $q_i q_j$, where $q_i \equiv g_i/\sqrt{|g_e g_p|}$. In particular, for the electron-proton system, the product of effective NP couplings can take the values $q_e q_p = \pm 1$. For $q_i q_j > 0$ the potential (2) is attractive (repulsive) for spin $0\,(1)$ mediator ϕ and vice versa for $q_i q_j < 0$.

In the numerical analysis, we consider the following benchmark NP models:

(a) Dark photon: The light NP mediator is a vector boson with couplings to the SM fermions proportional to their electric charges. A UV complete realization is an additional Abelian gauge boson with field strength $F'_{\mu\nu}$ that couples to the SM through the renormalizable kinetic mixing interaction, $-(\epsilon/2) F'_{\mu\nu} F^{\mu\nu}$ [22], where $F_{\mu\nu}$ is the electromagnetic field strength. To LO in ϵ this yields $\alpha_\phi = \alpha\epsilon^2$ and $q_e = q_\mu = -q_p = -1$, $q_n = 0$.

(b) $B - L$ gauge boson: The difference of baryon (B) and lepton (L) numbers is nonanomalous and can be gauged without introducing new fermions [23,24]. Light $B - L$ gauge boson with gauge coupling g_{B-L} gives rise to the NP potential in (2) with $\alpha_\phi = g_{B-L}^2/(4\pi)$. The charges $q_e = q_\mu = -q_p = -q_n = -1$ coincide with the dark photon ones, except for the neutron. Comparison of $B - L$ and dark photon bounds illustrates the importance of performing spectroscopy of different isotopes of the same species, such as hydrogen and deuterium.

(c) Scalar Higgs portal: A light scalar mixing with the Higgs boson [25,26] inherits the SM Yukawa structure, giving $\alpha_\phi = \sin^2\theta m_e \kappa_p m_p/(4\pi v^2) \lesssim 1.8 \times 10^{-10}$ where $v \simeq 246$ GeV is the SM Higgs vacuum expectation value, and θ is the scalar mixing angle. The effective leptonic ($\ell = e,\ \mu$) charges are $q_\ell = m_\ell/\sqrt{m_e \kappa_p m_p}$, while the effective nucleon charges ($N = p,\ n$) are given by $q_N = \kappa_N m_N/\sqrt{m_e \kappa_p m_p}$ with $\kappa_p \simeq 0.306(14)$ and $\kappa_n \simeq 0.308(14)$ [27–32] (see Supplemental Material [33]). Since couplings to muons and nucleons are enhanced by $q_\mu/q_e = m_\mu/m_e \simeq 200$ and $g_N/q_e = m_N/m_e \simeq 2 \times 10^3$, respectively, this NP benchmark highlights the relevance of muonic atom and molecular spectroscopy.

(d) Hadrophilic scalar: A scalar with $q_\ell = 0$ and $q_N = \kappa_N m_N/\sqrt{m_e \kappa_p m_p}$, i.e., with vanishing couplings to leptons, highlights the importance of molecular hydrogen ion spectroscopy as a probe of internuclear interactions [11,14]. For expedience, we take g_N to be the same as for the Higgs portal, but this could be relaxed in general.

(e) Up-lepto-darko-philic (ULD) scalar: In order to evade strong bounds from $K^+ \to \pi^+ + X_{\text{inv}}$ searches, where X_{inv} are invisible particles that escape the detector, see below, we adopt a particular version of a light scalar benchmark. The ULD scalar has enhanced couplings to leptons, $q_\ell = m_\ell/\sqrt{m_e \kappa'_p m_p}$, and reduced couplings to nucleons (due to couplings to only the up quark), $q_N = \kappa'_N m_N/\sqrt{m_e \kappa'_p m_p}$, with $\kappa'_p \simeq 0.018(5)$ and $\kappa'_n \simeq 0.016(5)$, and $\alpha_\phi = k^2 m_e \kappa'_p m_p/(4\pi v^2)$, with k a dimensionless parameter controlling the overall strength of interactions, which is varied in the fit. The ϕ is assumed to predominantly decay to invisible states, possibly related to the dark matter, which evades constraints from beam dump experiments. See Supplemental Material for further details [33], including results for an additional NP benchmark model—the scalar photon.

Datasets.—The adjustment of parameters, i.e., the fitting procedure, presented in this Letter has been carried out using two different datasets, CODATA18 and DATA22. The CODATA18 dataset consists of data that were used in the latest CODATA adjustment in Ref. [1], but restricted only to the subset most relevant for constraining NP. This subset contains observables related to the determination of the Rydberg constant R_∞, the proton and deuteron radii r_p and r_d, respectively, the fine-structure constant α, and the relative atomic masses of the electron, proton, and deuteron: $A_\mathrm{r}(e)$, $A_\mathrm{r}(p)$, and $A_\mathrm{r}(d)$, respectively. The inputs including theory uncertainties are listed in the Supplemental Material [33]. The other observables and parameters included in the CODATA 2018 adjustment are very weakly correlated with the selected data and can be neglected for our purpose.

The DATA22 dataset combines the updated CODATA18 inputs with the additional data that improve the overall sensitivity to NP (see Supplemental Material for details [33]). In particular, we include the measurements of transition frequencies in simple molecular or moleculelike systems, the hydrogen deuteride molecular ion (HD^+) [34–36], and the antiprotonic helium atom ($\bar{p}^3$He and $\bar{p}^4$He) [37,38]. These have an enhanced sensitivity to the NP models with mediators that have large couplings to quarks (and thus nuclei). The three benchmark models of this type are the Higgs portal, hadrophilic, and ULD scalars, see above.

The CODATA18 dataset is used as a reference point to verify the implementation of the inputs and the adjustment procedure, while DATA22 is used to obtain our nominal results. The full list of data in the two datasets, as well as further discussion of the importance of including certain observables when constraining NP, is given in the Supplemental Material [33], which includes Refs. [39–92].

Least-squares adjustment with new physics.—The experimental data are compared to the theoretical predictions with NP following the linearized least-squares procedure [93]. The theoretical prediction for an observable $\mathcal{O}$ takes the form

$$\mathcal{O} = \mathcal{O}_\mathrm{SM}(g_\mathrm{SM}) + \mathcal{O}_\mathrm{NP}(g_\mathrm{SM}, \alpha_\phi, m_\phi) + \delta\mathcal{O}_\mathrm{th}, \tag{3}$$

where $\mathcal{O}_\mathrm{SM}$ is the state-of-the-art SM prediction and depends on the SM parameters $g_\mathrm{SM} = \{R_\infty, r_p, r_d, \alpha, A_\mathrm{r}(e), A_\mathrm{r}(p), A_\mathrm{r}(d)\}$, while the NP contribution $\mathcal{O}_\mathrm{NP}$ depends in addition on α_ϕ and m_ϕ. The theoretical uncertainties are included as in Ref. [1], by adding a normally distributed variable $\delta\mathcal{O}_\mathrm{th}$ with zero mean and standard deviation equal to the estimated uncertainty of the theoretical expression. The $\delta\mathcal{O}_\mathrm{th}$'s are treated as yet another set of input data and varied in the fit, along with g_SM, α_ϕ, and m_ϕ, in order to minimize the χ^2 function constructed from the input data and theory predictions (see Supplemental Material [33]).

The SM theoretical predictions for atomic transition frequencies, the electron anomalous magnetic moment, and bound-electron g factors are from Ref. [1] (see references therein). The predictions for the HD^+ and $\bar{p}$He transition frequencies are from Refs. [94,95] and [96–98], respectively, and are updated with the latest CODATA recommended values, see Supplemental Material for details [33].

The NP contributions to atomic and molecular ion transition frequencies are obtained using (time-independent) first-order perturbation theory [99,100]. We use exact nonrelativistic wave functions for hydrogenlike atoms and very precise nonrelativistic numerical ones from a variational method of Ref. [101] for HD^+ and $\bar{p}$He. Expectation values of the Yukawa potentials in Eq. (2) are calculated for a grid of m_ϕ values, taking advantage of the fact that their matrix elements in the chosen basis can be obtained in an analytical form. The precision is limited to $\mathcal{O}(\alpha^2)$ because of the neglected relativistic corrections to the wave function. The NP contribution to the free electron $(g-2)_e$ arises at one loop [102,103], while for bound electrons we include an additional tree-level contribution from electron-nucleus interaction [104]. Finally, we assume NP to have negligible effects in atom recoil measurements as well as relative atomic mass measurements from cyclotron frequency measurements in Penning traps.

We pay particular attention to the possible degeneracy between the determination of SM and NP parameters. In the $m_\phi \to 0$ limit, the dark photon is completely degenerate with the QED photon, since couplings of the two are aligned, $q_i = Q_i$, and thus only the combination $\alpha + \alpha_\phi$ can be determined from data. This degeneracy should be retained in the theoretical predictions (3), which, in principle, requires calculating NP effects to the same very high order as the SM. We propose an alternative procedure, which uses the state-of-the-art SM calculations but requires NP contribution only at LO in α_ϕ and reproduces the correct $q_i \to Q_i$, $m_\phi a_0 \ll 1$ limit, where $a_0 \equiv \alpha/(4\pi R_\infty) = (\alpha m_e)^{-1}$ is the Bohr radius.

For "light vectors" we rewrite the NP potential in Eq. (2) as the sum of the Coulomb-like potential with QED coupling Q_i plus the remainder,

$$V_\mathrm{NP}^{ij}(r) = \alpha_\phi \frac{Q_i Q_j}{r} + \tilde{V}_\mathrm{NP}^{ij}(r), \tag{4}$$

where $\tilde{V}_\mathrm{NP}^{ij}(r) \equiv \alpha_\phi (q_i q_j e^{-m_\phi r} - Q_i Q_j)/r$. The theory predictions are evaluated at LO in $\tilde{V}_\mathrm{NP}(r)$, while the NP Coulomb term and the related relativistic corrections are evaluated to the same order as the SM, which amounts to replacing $\alpha \to \alpha + \alpha_\phi$ in the SM predictions. For any observable $\mathcal{O}$, the theoretical prediction is then

$$\mathcal{O} = \mathcal{O}_\mathrm{SM}(\alpha + \alpha_\phi) + \tilde{\mathcal{O}}_\mathrm{NP}(\alpha + \alpha_\phi, \alpha_\phi, m_\phi), \tag{5}$$

where $\mathcal{O}_\mathrm{SM}$ is the SM contribution now expressed as a function of $\alpha + \alpha_\phi$ and $\tilde{\mathcal{O}}_\mathrm{NP}$ is the NP contribution from $\tilde{V}_\mathrm{NP}$. In the $m_\phi \to 0$, $q_i \to Q_i$ limit, the potential $\tilde{V}_\mathrm{NP}$ vanishes, and all theory predictions are the SM ones, but shifted by $\alpha \to \alpha + \alpha_\phi$. For massive dark photon with $m_\phi a_0 \ll 1$, the leading effect of $\tilde{V}_{\rm NP}$ is parametrically $\tilde{\mathcal{O}}_{\rm NP} \propto m_\phi^2$. Note that for massless $B-L$ the potential $\tilde{V}_{\rm NP}$ vanishes in hydrogen but not in deuterium where $\tilde{\mathcal{O}}_{\rm NP} \propto q_n$, thus breaking the degeneracy between the SM and NP contributions when $m_\phi \to 0$.

For "light scalars" there is no degeneracy with QED in the massless mediator limit; it is lifted by relativistic corrections. We can use directly the state-of-the-art SM predictions and simply add to them the NP contribution due to the potential (2) at LO, without any special treatments, see also Supplemental Material [33].

Results.—First, we perform the control fit, i.e., the least-squares adjustment assuming SM, based on the CODATA18 dataset with inflated experimental uncertainties when there are tensions in the data [1], see also Supplemental Material [33]. The resulting χ^2 per degree of freedom (d.o.f.) is $\chi^2_{\rm SM}/\nu_{\rm d.o.f.} \simeq 0.95$ ($\nu_{\rm d.o.f.} = 78 - 44 = 34$), indicating an overall good description by the SM and the use of correct expansion factors. The output $g_{\rm SM}$ values and relative uncertainties (see Supplemental Material [33]) are in excellent agreement ($\lesssim 0.2\sigma$) with the latest CODATA recommended values [1], validating our procedure.

Next, we perform adjustments based on the DATA22 dataset, assuming either the SM or one of the above NP benchmark models. We do not inflate experimental errors, since mild tensions in the data could be a hint of NP. The SM-only hypothesis still describes the data relatively well, with $\chi^2_{\rm SM}/\nu_{\rm d.o.f.} \simeq 1.4$ ($\nu_{\rm d.o.f.} = 102 - 62 = 40$), despite known tensions in the proton charge radius puzzle data and the recent hydrogen $2S_{1/2} - 8D_{5/2}$ transition [20].

Figure 1 shows the 95% confidence level (C.L.) upper bounds on α_ϕ as function of m_ϕ for the NP benchmark models. The strongest exclusion is always reached around $m_\phi \sim a_0^{-1} \sim 4$ keV and stays roughly constant for lighter m_ϕ (except for dark photon due to degeneracy with QED in the $m_\phi \to 0$ limit, see above). Deuterium observables translate to a $\sim 2\times$ stronger bound on $B-L$ at $m_\phi \sim a_0^{-1}$, compared to dark photon. The significantly stronger bounds on the Higgs portal and hadrophilic scalar for $m_\phi \lesssim 10$ keV are due to the $\sim \kappa_p m_p/m_e \simeq 500$ enhancement in internucleon interactions (compared to electron-nucleon potential), affecting the HD$^+$ observables. For heavier NP, $m_\phi a_0 \gtrsim 1(m_\mu/m_e)$ in hydrogen (muonic hydrogen), the interaction is pointlike, with suppressed electron (muon) wave function overlap, and the bounds decouple as $\propto 1/m_\phi^2$ (and more quickly for hadrophilic scalar). The bounds are stronger for Higgs portal and ULD scalar due to $\sim m_\mu/m_e \simeq 200$ enhanced effects in muonic hydrogen.

For $m_\phi a_0 \gtrsim m_\mu/m_e$ the Higgs portal and ULD scalar are statistically preferred over the SM at the $\sim 4\sigma$ and $\sim 5\sigma$ level, respectively. Figure 2 shows the preferred region for the ULD scalar, around the best-fit point $m_\phi = 300$ keV and $\alpha_\phi = 6.7 \times 10^{-11}$. This NP hint is supported mostly from the recent measurements of the hydrogen $2S_{1/2} - 8D_{5/2}$ and $1S_{1/2} - 3S_{1/2}$ transitions [20,21], as well as muonic deuterium, cf. Supplemental Material [33]. While these tensions between data and the SM prediction are not new, our analysis shows that all tensions can be significantly ameliorated when including NP interactions due to a single

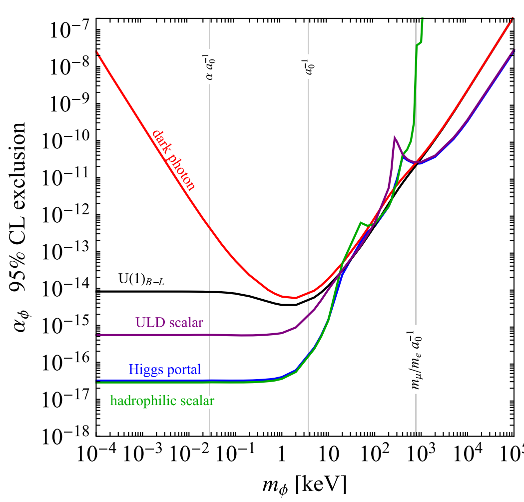

FIG. 1. The 95% C.L. bounds on the NP coupling constant α_ϕ as a function of the new boson's mass m_ϕ for the benchmark NP models as indicated. Other model-dependent constraints may apply (see text).

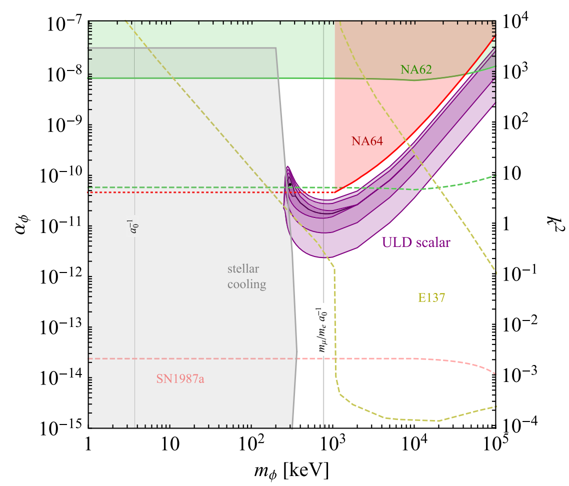

FIG. 2. The constraints on ULD scalar in the α_ϕ, m_ϕ plane, with purple-shaded 1, 2, 3, 4σ C.L. regions favored by the DATA22 dataset (black dot is the best-fit point). Exclusions are by SN1987a [105,106] (below the pink line, absent if ϕ invisible decay dominates), NA62 $K^+ \to \pi^+ X_{\rm inv}$ search [107] (green, the dashed line is a naive next-to-next-to-leading-order estimate), stellar cooling [108] (gray), NA64 $eZ \to eZX$ search [109] (red, dashed line is a naive extrapolation), and E137 [110,111] (between yellow dashed lines, absent if ϕ invisible decay dominates).

light scalar. The favored NP mass is close to the (inverse) Bohr radius of muonic atoms, $a_0^{-1} \times m_\mu/m_e \sim$ MeV, due to the large muon-electron coupling ratio in these models, contrasting with scalars having weaker or vanishing coupling to muons (see [20] and the Supplemental Material [33]).

However, other constraints require the scalar to have rather a nontrivial pattern of couplings, see the Supplemental Material [33]. For the ULD scalar, the E137 [110,111] bounds are evaded since ϕ decays predominantly to an invisible dark sector. Since ϕ couples to up quarks and not directly to heavy quarks and gluons, the bound from the NA62 search for $K^+ \to \pi^+\phi$ [107] is weakened [106,112]. The NA64 $eZ \to eZX$ search [109], naively extrapolated to low masses, excludes the best-fit point for the considered benchmark (see also [113]). However, this statement relies on the ratio of couplings to leptons and quark and is relaxed for somewhat larger couplings to quarks. Finally, the minimal ULD model induces a too large contribution to $(g-2)_\mu$, however, this can be suppressed in less minimal versions with a custodial symmetry [114].

The presence of NP also impacts the determination of the fundamental constants in the SM. Figure 3 shows the 68% C.L. determination of r_p and R_∞, subtracting the CODATA 2018 recommended values and normalizing to respective errors. The SM-parameter uncertainties increase in the presence of NP and the central values shift outside the nominal SM ellipse, shown explicitly in Fig. 3 for the Higgs portal and ULD scalar model. Because of the degeneracy with the photon, the uncertainty on α in the dark photon model increases as $1/m_\phi^2$ for masses below 10 eV (see Supplemental Material [33]) and eventually becomes comparable to α itself for $m_\phi \sim 0.1$ meV, while $\alpha + \alpha_\phi$ remains well constrained.

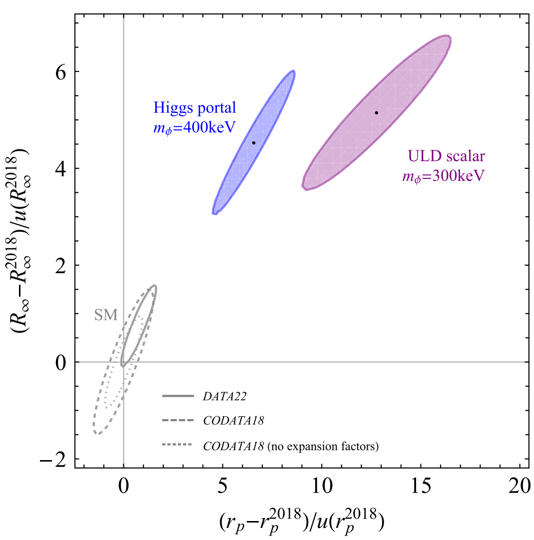

FIG. 3. The 68% C.L. regions for simultaneous determinations of the Rydberg constant R_∞ and the proton radius r_p assuming either the SM-only hypothesis (gray) or including putative NP contributions from a 400 keV Higgs portal scalar (blue) or 300 keV ULD scalar (purple). The solid lines use the DATA22 dataset; the dashed (dotted) lines use the CODATA18 dataset with (without) errors inflated by expansion factors. Both R_∞ and r_p are shown in terms of normalized deviations from the central values of the CODATA 2018 analysis, Ref. [1].

Conclusions.—Extracting bounds on light NP from a global fit to spectroscopic and other precision data requires both SM and NP parameters to be determined simultaneously. The possibility of NP contributions changes the extracted allowed ranges of SM parameters, a change that can be quite substantial, see Fig. 3. Furthermore, we provided a prescription to consistently include NP corrections from light vectors. It requires calculations of NP contribution only at leading order and recovers the expected degeneracy between dark photon and QED in the massless mediator limit.

At present, spectroscopic data show tensions that could either be due to unknown or underappreciated systematics or to light NP. We showed that the $\sim 4\sigma$ anomaly in data can be explained by a flavor nonuniversal light scalar model.

We would like to thank Dmitry Budker and Gilad Perez for useful discussions and comments on the Letter. The work of C. D. is supported by the CNRS IRP NewSpec. The work of T. K. is supported by the Japan Society for the Promotion of Science (JSPS) Grant-in-Aid for Early-Career Scientists (Grant No. 19K14706) and the JSPS Core-to-Core Program (Grant No. JPJSCCA20200002). The work of Y. S. is supported by grants from the NSF-BSF (No. 2018683), the ISF (No. 482/20), the BSF (No. 2020300), and by the Azrieli foundation. J. Z. acknowledges support in part by the DOE Award No. de-sc0011784. This work was also supported in part by the European Union's Horizon 2020 research and innovation program, project STRONG2020, under Grant Agreement No. 824093.

*cedric.delaunay@lapth.cnrs.fr
†karr@lkb.upmc.fr
‡teppeik@kmi.nagoya-u.ac.jp
§j.c.j.koelemeij@vu.nl
‖soreqy@physics.technion.ac.il
¶zupanje@ucmail.uc.edu

[1] E. Tiesinga, P. J. Mohr, D. B. Newell, and B. N. Taylor, CODATA recommended values of the fundamental physical constants: 2018*, Rev. Mod. Phys. **93**, 025010 (2021).

[2] D. Hanneke, S. Fogwell, and G. Gabrielse, New Measurement of the Electron Magnetic Moment and the Fine Structure Constant, Phys. Rev. Lett. **100**, 120801 (2008).

[3] Muon g-2 Collaboration, Measurement of the Positive Muon Anomalous Magnetic Moment to 0.46 ppm, Phys. Rev. Lett. **126**, 141801 (2021).

[4] ACME Collaboration, Improved limit on the electric dipole moment of the electron, Nature (London) **562**, 355 (2018).

[5] J. Jaeckel and S. Roy, Spectroscopy as a test of Coulomb's law: A probe of the hidden sector, Phys. Rev. D **82**, 125020 (2010).

[6] S. G. Karshenboim, Constraints on a long-range spin-independent interaction from precision atomic physics, Phys. Rev. D **82**, 073003 (2010).

[7] C. Delaunay, R. Ozeri, G. Perez, and Y. Soreq, Probing atomic Higgs-like forces at the precision frontier, Phys. Rev. D **96**, 093001 (2017).

[8] J. C. Berengut *et al.*, Probing New Long-Range Interactions by Isotope Shift Spectroscopy, Phys. Rev. Lett. **120**, 091801 (2018).

[9] C. Frugiuele, J. Pérez-Ríos, and C. Peset, Current and future perspectives of positronium and muonium spectroscopy as dark sectors probe, Phys. Rev. D **100**, 015010 (2019).

[10] C. Frugiuele and C. Peset, Muonic vs electronic dark forces: A complete EFT treatment for atomic spectroscopy, J. High Energy Phys. 05 (2022) 002.

[11] E. J. Salumbides, J. C. J. Koelemeij, J. Komasa, K. Pachucki, K. S. E. Eikema, and W. Ubachs, Bounds on fifth forces from precision measurements on molecules, Phys. Rev. D **87**, 112008 (2013).

[12] M. Borkowski, A. A. Buchachenko, R. Ciuryło, P. S. Julienne, H. Yamada, Y. Kikuchi, Y. Takasu, and Y. Takahashi, Weakly bound molecules as sensors of new gravitylike forces, Sci. Rep. **9**, 14807 (2019).

[13] S. Alighanbari, G. S. Giri, F. L. Constantin, V. I. Korobov, and S. Schiller, Precise test of quantum electrodynamics and determination of fundamental constants with HD + ions, Nature (London) **581**, 152 (2020).

[14] M. Germann, S. Patra, J.-Ph. Karr, L. Hilico, V. I. Korobov, E. J. Salumbides, K. S. E. Eikema, W. Ubachs, and J. C. J. Koelemeij, Three-body QED test and fifth-force constraint from vibrations and rotations of HD^+, Phys. Rev. Res. **3**, L022028 (2021).

[15] M. S. Safronova, D. Budker, D. DeMille, D. F. Jackson Kimball, A. Derevianko, and C. W. Clark, Search for new physics with atoms and molecules, Rev. Mod. Phys. **90**, 025008 (2018).

[16] M. P. A. Jones, R. M. Potvliege, and M. Spannowsky, Probing new physics using Rydberg states of atomic hydrogen, Phys. Rev. Res. **2**, 013244 (2020).

[17] R. Pohl *et al.*, The size of the proton, Nature (London) **466**, 213 (2010).

[18] A. Antognini *et al.*, Proton structure from the measurement of $2S-2P$ transition frequencies of muonic hydrogen, Science **339**, 417 (2013).

[19] J.-P. Karr, D. Marchand, and E. Voutier, The proton size, Nat. Rev. Phys. **2**, 601 (2020).

[20] A. D. Brandt, S. F. Cooper, C. Rasor, Z. Burkley, A. Matveev, and D. C. Yost, Measurement of the 2S1/2-8D5/2 Transition in Hydrogen, Phys. Rev. Lett. **128**, 023001 (2022).

[21] A. Grinin, A. Matveev, D. C. Yost, L. Maisenbacher, V. Wirthl, R. Pohl, T. W. Hänsch, and T. Udem, Two-photon frequency comb spectroscopy of atomic hydrogen, Science **370**, 1061 (2020).

[22] B. Holdom, Two U(1)'s and epsilon charge shifts, Phys. Lett. **166B**, 196 (1986).

[23] A. Davidson, $B-L$ as the fourth color within an $\mathrm{SU}(2)_L \times \mathrm{U}(1)_R \times \mathrm{U}(1)$ model, Phys. Rev. D **20**, 776 (1979).

[24] R. E. Marshak and R. N. Mohapatra, Quark-lepton symmetry and $B-L$ as the U(1) generator of the electroweak symmetry group, Phys. Lett. **91B**, 222 (1980).

[25] B. Patt and F. Wilczek, Higgs-field portal into hidden sectors, arXiv:hep-ph/0605188.

[26] D. O'Connell, M. J. Ramsey-Musolf, and M. B. Wise, Minimal extension of the standard model scalar sector, Phys. Rev. D **75**, 037701 (2007).

[27] M. A. Shifman, A. I. Vainshtein, and V. I. Zakharov, Remarks on Higgs boson interactions with nucleons, Phys. Lett. **78B**, 443 (1978).

[28] G. Belanger, F. Boudjema, A. Pukhov, and A. Semenov, Dark matter direct detection rate in a generic model with micrOMEGAs 2.2, Comput. Phys. Commun. **180**, 747 (2009).

[29] P. M. Junnarkar and A. Walker-Loud, Scalar strange content of the nucleon from lattice QCD, Phys. Rev. D **87**, 114510 (2013).

[30] G. Belanger, F. Boudjema, A. Pukhov, and A. Semenov, micrOMEGAs_3: A program for calculating dark matter observables, Comput. Phys. Commun. **185**, 960 (2014).

[31] F. Bishara, J. Brod, B. Grinstein, and J. Zupan, From quarks to nucleons in dark matter direct detection, J. High Energy Phys. 11 (2017) 059.

[32] F. Bishara, J. Brod, B. Grinstein, and J. Zupan, DirectDM: A tool for dark matter direct detection, arXiv: 1708.02678.

[33] See Supplemental Material at http://link.aps.org/supplemental/10.1103/PhysRevLett.130.121801 for further details on the linearized least squares method, the datasets used, the new physics benchmarks models, the new physics improvements relative to the standard model, the extraction of fundamental constants in the presence of new physics, and the massless limit for new physics vector states, which includes Refs. [38–92].

[34] S. Alighanbari, G. S. Giri, F. L. Constantin, V. I. Korobov, and S. Schiller, Precise test of quantum electrodynamics and determination of fundamental constants with HD^+ ions, Nature (London) **581**, 152 (2020).

[35] S. Patra, M. Germann, J.-Ph. Karr, M. Haidar, L. Hilico, V. I. Korobov, F. M. J. Cozijn, K. S. E. Eikema, W. Ubachs, and J. C. J. Koelemeij, Proton-electron mass ratio from laser spectroscopy of HD^+ at the part-per-trillion level, Science **369**, 1238 (2020).

[36] I. V. Kortunov, S. Alighanbari, M. G. Hansen, G. S. Giri, V. I. Korobov, and S. Schiller, Proton-electron mass ratio by high-resolution optical spectroscopy of ion ensembles in the resolved-carrier regime, Nat. Phys. **17**, 569 (2021).

[37] M. Hori *et al.*, Two-photon laser spectroscopy of antiprotonic helium and the antiproton-to-electron mass ratio, Nature (London) **475**, 484 (2011).

[38] M. Hori *et al.*, Buffer-gas cooling of antiprotonic helium to 1.5 to 1.7 K, and antiproton-to-electron mass ratio, Science **354**, 610 (2016).

[39] R. Bouchendira, P. Cladé, S. Guellati-Khélifa, F. Nez, and F. Biraben, New Determination of the Fine Structure Constant and Test of the Quantum Electrodynamics, Phys. Rev. Lett. **106**, 080801 (2011).
[40] R. H. Parker, C. Yu, W. Zhong, B. Estey, and H. Müller, Measurement of the fine-structure constant as a test of the standard model, Science **360**, 191 (2018).
[41] W. J. Huang, G. Audi, M. Wang, F. G. Kondev, S. Naimi, and X. Xu, The AME2016 atomic mass evaluation (I). Evaluation of input data; and adjustment procedures, Chin. Phys. C **41**, 030002 (2017).
[42] M. Wang, G. Audi, F. G. Kondev, W. J. Huang, S. Naimi, and X. Xu, The AME2016 atomic mass evaluation (II). Tables, graphs and references, Chin. Phys. C **41**, 030003 (2017).
[43] A. Kramida, Yu. Ralchenko, J. Reader, and NIST ASD Team, NIST Atomic Spectra Database (ver. 5.9), Available: https://physics.nist.gov/asd. National Institute of Standards and Technology, Gaithersburg, MD, 2021.
[44] F. Heiße *et al.*, High-Precision Measurement of the Proton's Atomic Mass, Phys. Rev. Lett. **119**, 033001 (2017).
[45] S. L. Zafonte and R. S. V. Dyck, Ultra-precise single-ion atomic mass measurements on deuterium and helium-3, Metrologia **52**, 280 (2015).
[46] V. A. Yerokhin, K. Pachucki, and V. Patkóš, Theory of the Lamb shift in hydrogen and light hydrogen-like ions, Ann. Phys. (Amsterdam) **531**, 1800324 (2019).
[47] S. G. Karshenboim, A. Ozawa, V. A. Shelyuto, R. Szafron, and V. G. Ivanov, The Lamb shift of the 1s state in hydrogen: Two-loop and three-loop contributions, Phys. Lett. B **795**, 432 (2019).
[48] R. Szafron, E. Y. Korzinin, V. A. Shelyuto, V. G. Ivanov, and S. G. Karshenboim, Virtual Delbrück scattering and the Lamb shift in light hydrogenlike atoms, Phys. Rev. A **100**, 032507 (2019).
[49] S. G. Karshenboim and V. A. Shelyuto, Three-loop radiative corrections to the 1s Lamb shift in hydrogen, Phys. Rev. A **100**, 032513 (2019).
[50] L. Morel, Z. Yao, P. Cladé, and S. Guellati-Khélifa, Determination of the fine-structure constant with an accuracy of 81 parts per trillion, Nature (London) **588**, 61 (2020).
[51] X. Fan, T. G. Myers, B. A. D. Sukra, and G. Gabrielse, Measurement of the Electron Magnetic Moment, Phys. Rev. Lett. **130**, 071801 (2023).
[52] A. Czarnecki, J. Piclum, and R. Szafron, Logarithmically enhanced Euler-Heisenberg Lagrangian contribution to the electron gyromagnetic factor, Phys. Rev. A **102**, 050801 (R) (2020).
[53] W. J. Huang, M. Wang, F. G. Kondev, G. Audi, and S. Naimi, The AME 2020 atomic mass evaluation (I). Evaluation of input data, and adjustment procedures, Chin. Phys. C **45**, 030002 (2021).
[54] M. Wang, W. J. Huang, F. G. Kondev, G. Audi, and S. Naimi, The AME 2020 atomic mass evaluation (II). Tables, graphs and references, Chin. Phys. C **45**, 030003 (2021).
[55] F. Heiße, S. Rau, F. Köhler-Langes, W. Quint, G. Werth, S. Sturm, and K. Blaum, High-precision mass spectrometer for light ions, Phys. Rev. A **100**, 022518 (2019).
[56] S. Rau, F. Heiße, F. Köhler-Langes, S. Sasidharan, R. Haas, D. Renisch, C. E. Düllmann, W. Quint, S. Sturm, and K. Blaum, Penning-trap mass measurements of the deuteron and the HD^+ molecular ion, Nature (London) **585**, 43 (2020).
[57] D. J. Fink and E. G. Myers, Deuteron-to-Proton Mass Ratio from the Cyclotron Frequency Ratio of H_2^+ to D^+ with H_2^+ in a Resolved Vibrational State, Phys. Rev. Lett. **124**, 013001 (2020).
[58] D. J. Fink and E. G. Myers, Deuteron-To-Proton Mass Ratio from Simultaneous Measurement of the Cyclotron Frequencies of H_2^+ and D^+, Phys. Rev. Lett. **127**, 243001 (2021).
[59] J. J. Krauth *et al.*, Measuring the alpha-particle charge radius with muonic helium-4 ions, Nature (London) **589**, 527 (2021).
[60] J. Krauth, The Lamb shift of the muonic helium-3 ion and the helion charge radius, Ph.D. thesis, Ludwig-Maximilians University, Munich, 2017.
[61] W. Xiong *et al.*, A small proton charge radius from an electron–proton scattering experiment, Nature (London) **575**, 147 (2019).
[62] Z.-F. Cui, D. Binosi, C. D. Roberts, and S. M. Schmidt, Fresh Extraction of the Proton Charge Radius from Electron Scattering, Phys. Rev. Lett. **127**, 092001 (2021).
[63] S. Schiller and V. Korobov, Tests of time independence of the electron and nuclear masses with ultracold molecules, Phys. Rev. A **71**, 032505 (2005).
[64] V. I. Korobov, Bethe logarithm for resonant states: Antiprotonic helium, Phys. Rev. A **89**, 014501 (2014).
[65] D. T. Aznabayev, A. K. Bekbaev, and V. I. Korobov, Leading-order relativistic corrections to the rovibrational spectrum of H_2^+ and HD^+ molecular ions, Phys. Rev. A **99**, 012501 (2019).
[66] V. I. Korobov, Metastable states in the antiprotonic helium atom decaying via Auger transitions, Phys. Rev. A **67**, 062501 (2003).
[67] V. I. Korobov and Z.-X. Zhong, Bethe logarithm for the H_2^+ and HD^+ molecular ions, Phys. Rev. A **86**, 044501 (2012).
[68] V. I. Korobov, Leading-order relativistic and radiative corrections to the rovibrational spectrum of H2+ and HD+ molecular ions, Phys. Rev. A **74**, 052506 (2006).
[69] V. I. Korobov, Calculation of transitions between metastable states of antiprotonic helium including relativistic and radiative corrections of order $R_\infty \alpha^4$, Phys. Rev. A **77**, 042506 (2008).
[70] V. I. Korobov and T. Tsogbayar, Relativistic corrections of order $m\alpha^6$ to the two-centre problem, J. Phys. B **40**, 2661 (2007).
[71] K. Pachucki, Recoil Effects in Positronium Energy Levels to Order α^6, Phys. Rev. Lett. **79**, 4120 (1997).
[72] K. Pachucki, Radiative recoil correction to the Lamb shift, Phys. Rev. A **52**, 1079 (1995).
[73] A. Czarnecki and K. Melnikov, Expansion of Bound-State Energies in Powers of m/M, Phys. Rev. Lett. **87**, 013001 (2001).
[74] T. Tsogbayar and V. I. Korobov, Relativistic correction to the $1s\sigma$ and $2p\sigma$ electronic states of the H_2^+ molecular ion

and the moleculelike states of the antiprotonic helium $He^+\bar{p}$, J. Chem. Phys. **125**, 024308 (2006).
[75] V. I. Korobov, L. Hilico, and J.-P. Karr, Theoretical transition frequencies beyond 0.1 ppb accuracy in H_2^+, HD^+, and antiprotonic helium, Phys. Rev. A **89**, 032511 (2014).
[76] V. I. Korobov, L. Hilico, and J.-P. Karr, Bound-state QED calculations for antiprotonic helium, Hyperfine Interact. **233**, 75 (2015).
[77] J. P. Karr, L. Hilico, and V. I. Korobov, One-loop vacuum polarization at $m\alpha^7$ and higher orders for three-body molecular systems, Phys. Rev. A **95**, 042514 (2017).
[78] A. Crivellin, M. Hoferichter, and M. Procura, Accurate evaluation of hadronic uncertainties in spin-independent WIMP-nucleon scattering: Disentangling two- and three-flavor effects, Phys. Rev. D **89**, 054021 (2014).
[79] Flavour Lattice Averaging Group, FLAG Review 2019: Flavour Lattice Averaging Group (FLAG), Eur. Phys. J. C **80**, 113 (2020).
[80] xQCD Collaboration, πN and strangeness sigma terms at the physical point with chiral fermions, Phys. Rev. D **94**, 054503 (2016).
[81] MILC Collaboration, Intrinsic strangeness and charm of the nucleon using improved staggered fermions, Phys. Rev. D **88**, 054503 (2013).
[82] S. Durr *et al.*, Lattice Computation of the Nucleon Scalar Quark Contents at the Physical Point, Phys. Rev. Lett. **116**, 172001 (2016).
[83] S. Durr *et al.*, Sigma term and strangeness content of octet baryons, Phys. Rev. D **85**, 014509 (2012); **93**, 039905(E) (2016).
[84] C. Alexandrou *et al.*, Nucleon axial, tensor, and scalar charges and σ-terms in lattice QCD, Phys. Rev. D **102**, 054517 (2020).
[85] S. Borsanyi *et al.*, Ab-initio calculation of the proton and the neutron's scalar couplings for new physics searches, arXiv:2007.03319.
[86] W. Altmannshofer, S. Gori, A. L. Kagan, L. Silvestrini, and J. Zupan, Uncovering Mass Generation through Higgs Flavor Violation, Phys. Rev. D **93**, 031301(R) (2016).
[87] F. J. Botella, G. C. Branco, M. Nebot, and M. N. Rebelo, Flavour changing Higgs couplings in a class of two Higgs doublet models, Eur. Phys. J. C **76**, 161 (2016).
[88] D. Ghosh, R. S. Gupta, and G. Perez, Is the Higgs mechanism of fermion mass generation a fact? A Yukawa-less first-two-generation model, Phys. Lett. B **755**, 504 (2016).
[89] CMS Collaboration, Evidence for Higgs boson decay to a pair of muons, J. High Energy Phys. 01 (2021) 148.
[90] N. Bar, K. Blum, and G. D'Amico, Is there a supernova bound on axions?, Phys. Rev. D **101**, 123025 (2020).
[91] P. S. B. Dev, R. N. Mohapatra, and Y. Zhang, Revisiting supernova constraints on a light CP-even scalar, J. Cosmol. Astropart. Phys. 08 (2020) 003; 11 (2020) E01.
[92] H. Gao and M. Vanderhaeghen, The proton charge radius, Rev. Mod. Phys. **94**, 015002 (2022).
[93] P. J. Mohr and B. N. Taylor, CODATA recommended values of the fundamental physical constants: 1998, Rev. Mod. Phys. **72**, 351 (2000).
[94] V. I. Korobov, L. Hilico, and J. P. Karr, Fundamental Transitions and Ionization Energies of the Hydrogen Molecular Ions with Few ppt Uncertainty, Phys. Rev. Lett. **118**, 233001 (2017).
[95] V. I. Korobov and J. P. Karr, Rovibrational spin-averaged transitions in the hydrogen molecular ions, Phys. Rev. A **104**, 032806 (2021).
[96] V. I. Korobov, Calculation of transitions between metastable states of antiprotonic helium including relativistic and radiative corrections of order $R_\infty\alpha^4$, Phys. Rev. A **77**, 042506 (2008).
[97] V. I. Korobov, Bethe logarithm for resonant states: Antiprotonic helium, Phys. Rev. A **89**, 014501 (2014).
[98] V. I. Korobov, L. Hilico, and J.-P. Karr, mα^7 -Order Corrections in the Hydrogen Molecular Ions and Antiprotonic Helium, Phys. Rev. Lett. **112**, 103003 (2014).
[99] C. Cohen-Tannoudji, B. Diu, and F. Laloë, *Quantum Mechanics*; 1st ed. (Wiley, New York, 1977); Translation of *Mécanique Quantique* (Hermann, Paris, 1973).
[100] A. Messiah, *Quantum Mechanics* (Dover Publications, New York, 2014).
[101] V. I. Korobov, Coulomb three-body bound-state problem: Variational calculations of nonrelativistic energies, Phys. Rev. A **61**, 064503 (2000).
[102] R. Jackiw and S. Weinberg, Weak interaction corrections to the muon magnetic moment and to muonic atom energy levels, Phys. Rev. D **5**, 2396 (1972).
[103] F. Jegerlehner and A. Nyffeler, The muon $g-2$, Phys. Rep. **477**, 1 (2009).
[104] V. Debierre, C. H. Keitel, and Z. Harman, Fifth-force search with the bound-electron g factor, Phys. Lett. B **807**, 135527 (2020).
[105] G. Raffelt, Limits on a CP-violating scalar axion-nucleon interaction, Phys. Rev. D **86**, 015001 (2012).
[106] B. Batell, A. Freitas, A. Ismail, and D. McKeen, Probing light dark matter with a hadrophilic scalar mediator, Phys. Rev. D **100**, 095020 (2019).
[107] NA62 Collaboration, Measurement of the very rare $K^+ \to \pi^+\nu\bar{\nu}$ decay, J. High Energy Phys. 06 (2021) 093.
[108] E. Hardy and R. Lasenby, Stellar cooling bounds on new light particles: Plasma mixing effects, J. High Energy Phys. 02 (2017) 033.
[109] NA64 Collaboration, Constraints on New Physics in Electron $g-2$ from a Search for Invisible Decays of a Scalar, Pseudoscalar, Vector, and Axial Vector, Phys. Rev. Lett. **126**, 211802 (2021).
[110] J. D. Bjorken *et al.*, Search for neutral metastable penetrating particles produced in the SLAC beam dump, Phys. Rev. D **38**, 3375 (1988).
[111] Y.-S. Liu, D. McKeen, and G. A. Miller, Validity of the Weizsäcker-Williams approximation and the analysis of beam dump experiments: Production of a new scalar boson, Phys. Rev. D **95**, 036010 (2017).
[112] C. Delaunay *et al.* (to be published).
[113] *BABAR* Collaboration, Search for Invisible Decays of a Dark Photon Produced in e^+e^- Collisions at *BaBar*, Phys. Rev. Lett. **119**, 131804 (2017).
[114] R. Balkin, C. Delaunay, M. Geller, E. Kajomovitz, G. Perez, Y. Shpilman, and Y. Soreq, Custodial symmetry for muon $g-2$, Phys. Rev. D **104**, 053009 (2021).